

Zinc oxide coated polymer optical fiber for measuring uric acid concentrations

A. R. A. RASHID^{a,b,*}, N. A. F. SHAMSURI^a, A. H. SURANI^a, A. A. N. HAKIM^a, K. ISMAIL^c

^aFaculty of Science and Technology, Universiti Sains Islam Malaysia, 71800 Nilai, Negeri Sembilan, Malaysia

^bFrontier Materials Research Group (FMRG), Faculty of Science and Technology, Universiti Sains Islam Malaysia (USIM), Bandar Baru Nilai, Negeri Sembilan, Malaysia

^cDepartment of Electrical & Electronics Engineering, Faculty of Engineering, Universiti Pertahanan Nasional Malaysia, Kuala Lumpur 57000, Malaysia

Uric acid detection based on ZnO coated polymer optical fiber (POF) by using intensity modulation technique is proposed. Zinc oxide was prepared using sol-gel method and characterized using UV-Vis spectrometer in order to determine its optical properties such as transmittance, absorbance and refractive index. The POF cladding is removed by using acetone and the unclad length of 2 cm was coated with ZnO by using dip coating method. The unclad fiber without coating is tested under uric acid solutions for comparison purpose. As the uric acid concentration increases until 500 ppm, the power output increases for ZnO coated fiber and produces a sensitivity of 4×10^{-6} mW/ppm with a slope linearity of more than 88.56 %. The refractive index of ZnO is changing due to the interaction with uric acid and allows more light to propagate inside the fiber. The sensitivity for 2 cm and 4 cm of uncoated fiber is 2×10^{-6} mW/ppm and 7×10^{-6} mW/ppm. The longer the length of unclad fiber, the higher the evanescent wave absorbance as well as the number of reflections inside the fiber.

(Received May 28, 2018; accepted February 12, 2019)

Keywords: Polymer optical fiber, Zinc oxide, Uric acid

1. Introduction

Uric acid is a main nitrogenous complex which is represented by the formula of $C_5H_4N_4O_3$. Moreover, this compound is produced from metabolic conversion of purines, primarily in the liver, muscle, and intestine [1]. Hence, it is deemed crucial to monitor the concentration of uric acid dissipated in human urine and plasma considering the fact that any elevated level of uric acid in blood plasma will cause various diseases such as atherosclerotic cardiovascular disease, peripheral artery disease, and chronic kidney disease [2]. As a result, the needs to sense uric acid has highly increased. Apart from that, there are several methods that can be employed in detecting uric acid which include amperometric sensor, potentiometer, and zinc oxide (ZnO) nanowires. Moreover, the amperometric biosensors are useful in detecting oxygen consumption, chemiluminescence, and fluoride ions. In this technique, the electrodes are required to be placed approximately at 0.7 V because this is a suitable value for the surface of the electrode that allows the reaction of biological electro active molecules to occur. On a more important note, the potentiometer is created based on ZnO nanoflakes and immobilized uricase. However, it should be noted the sensitivity of ion towards electrodes is limited because it is only capable of sensing charged ions [3].

In relation to this matter, ZnO has attracted a considerable amount of attention due to its unique properties which include a wide semiconducting compound that possesses a direct band gap of 3.37 eV as

well as greater excitation binding energy of 60 meV [4]. Moreover, ZnO is also thermally stable to extremely high temperature (at least 1800 °C), while the larger value allows the excitonic transition to take place in case the ZnO can potentially occur at room temperature [5]. Meanwhile, ZnO also has high transmittance and good electrical conductivity [6]. In addition, ZnO tends to offer a significant material for UV optoelectronic devices because it has large excitation binding energy [7]. More importantly this material can be extensively used in VOC sensor [8], ultraviolet sensor [9], piezoelectric transducers, varistors, optical coatings, and thin film solar cells due to the outstanding piezoelectric, optical, and electronic properties [7].

In regard to this matter, optical fiber (POF) is known to have similar structure as the glass optical fibers which include core, cladding, and jacket. On another note, POF has been reported to attract the attention of researchers because it acts as an alternative for the glass optical fiber (GOF) in particular areas [10]. POF offers more advantages which include the ease of joining, potential negative thermo-optic coefficient [11], easy to handle, good flexibility, immune to electromagnetic interferences [12], lower density, and higher elastic deformation limits compared to glass optical fiber. The differences between plastic optical fiber from others optical fibers refers to the material that made up the core which is polymethylmethacrylate (PMMA) with the normal radius around 125-409 μm [11]. Moreover, there are several optical plastic that are used in the fabrication of POF apart from PMMA, namely amorphous fluorinated polymer

(CYTOP), polystyrene (PS), and polycarbonate (PC) [13]. The larger diameter of POF makes it easy to be handled, cleaved, and joined. On a more important note, plastic optical fiber is useful in bioengineering [14], chemical detection [14], sensor distribution [16], data transmission at short distance which include Fiber to The Home (FTTH) [17] and Media Oriented Systems Transport (MOST) in automobile system [10].

The usage of fiber optic as sensors has been widely studied in the field of chemistry and physics. Generally, polymer optical fiber has been adopted for nitrite detection which acts as the initial level study towards the progress of oral cancer sensor [18]. On a similar note, fiber optic has been often chosen as a chemical sensor in verifying cations and anions due to its low cost, easy fabrication, and greater sensitivity and selectivity [19]. In addition, POF sensors are frequently endorsed to be less expensive and easier to set up compared to glass optical fiber. The characteristics of optical fiber as a biosensor which include very petite, flexible, and weightless make it a suitable choice to insert catheters and needles to measure inner tissue and plasma. Moreover, there are a few types of sensor based on POF that are coated with specific materials which are used in humidity measurement [20], detection of gas [21], and liquid level [22]. In this context of humidity measurement, POF is coated with polymer blend of hydroxyethylcellulose or polyvinylidene fluoride (HEC/PVDF), in which the sensor shows that the coating material tends to change the conductance when it reacts with humidity. Meanwhile, in the case of gas detection, POF is coated with silver nanoparticles/PVP/PVA hybrid and then analyzed with the detection of gas such as ammonia, methanol, and ethanol. In this paper, the effect of uric acid concentration on ZnO coated POF fiber optic is reported and discussed.

2. Methodology

The experimental procedure for this experiment consisted of two parts, in which the first part refers to the preparation of ZnO and the characterization of ZnO using UV-Vis spectrometer. Meanwhile, the second part involves the preparation of unclad POF, the coating of ZnO to the unclad POF, and the coupling of POF to the light source and optical power meter.

ZnO was synthesized using sol gel method. The solution was prepared by mixing zinc acetate dehydrate with isopropanol with the concentration of 0.03 M respectively. Next, the temperature was set to 60 °C for 2 hours, while the solution was stirred on magnetic stirrer to produce a clear and homogenous solution. Moreover, the solution was cooled down to room temperature for coating purposes. On another note, the characterization of ZnO oxide was performed using UV-Vis spectrometer in order to obtain the optical properties. The scanning of absorption was carried out using single beam of UV-Vis spectrometer. In addition, the absorption of UV-Vis light for sample of ZnO was compared to the blank based on the

baseline correction. The absorbance data for wavelength from 300 nm to 800 nm was recorded.

The next step involved the process of preparing and coating ZnO to the unclad POF. In this study, the chemical etching method was adopted to unclad the POF which requires the use of several materials and equipments, namely acetone, deionized water, and sand paper. The first step required the jacket to be removed according to the required length which is 0.02 m and 0.04 m. Then, the POF fiber was etched using acetone solution and then neutralized with distilled water. The acetone applied will react with POF to form milky foam on cladding which was then removed using sand paper. In this case, the process was repeated until the unclad POF has a diameter of ± 0.85 mm measured using digital vernier caliper. Finally, the unclad POF was cleaned again with distilled water. Meanwhile, the fiber was manually dip into the solution and dried at 50 °C for 10 min to vaporise the solvent and eliminate organic residuals for the purpose of coating the unclad POF with ZnO. This coating and drying method was repeated for five times to increase the thickness of the fibers. In this experiment, uric acid was first diluted in the distilled water to obtain the concentration of 100 ppm, 200 ppm, 300 ppm, 400 ppm, and 500 ppm. In this case, the setup consisted of probe, LED source, and power meter for the proposed sensor in order to detect different uric acid concentration.

3. Discussion

3.1. Synthesis and characterization of zinc oxide

In the current experiment, ZnO was synthesized using sol gel method that required zinc acetate dehydrate to be dissolved in the isopropanol. The absorbance measurement must be recorded from 300 nm to 800 nm wavelength range, in which the bulk absorption of ZnO should appear at 380 nm theoretically [23]. However, as can be observed in Fig. 1 regarding the absorbance spectrum of ZnO against wavelength, the result showed that ZnO tends to exhibit a strong absorption band which is blue shifted at 340 nm with respect to the bulk absorption. In this context, blue shift refers to the absorption that is shifted to lower wavelength but with higher energy. Hence, it should be noted that the slight shift in the absorption is caused by the change in particle size or particle shape [24].

The size of ZnO nanoparticles from the absorbance spectra can be determined using Equation 1 that is derived from the effective mass model [25].

$$r(\text{nm}) = \frac{-0.3049 + \sqrt{-26.23012 + \frac{10240.72}{\lambda_p(\text{nm})}}}{-6.3829 + \frac{2483.2}{\lambda_p(\text{nm})}} \quad (1)$$

In this case, the value used throughout the derivation of Equation 1 is $m_e = 0.26$, $m_h = 0.59$, m_0 which is free electron mass, $\epsilon = 8.5$ and $E_g = 3.3$ eV. The synthesized ZnO displays the peak absorbance at 340 nm with the particle size of 3.62 nm that is smaller than the average size value of 5-8 nm [24].

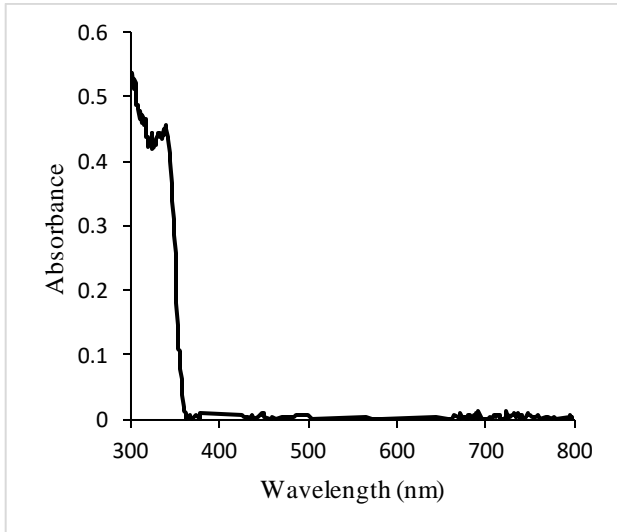


Fig. 1. UV-Vis the absorbance spectrum of ZnO nanoparticles

Another important optical properties of ZnO is the transmittance percentage against the wavelength. A few studies have reported that ZnO exhibits high transmission $\geq 70\%$ because it is a semiconductor that has a wide direct band gap. This is corresponding with the data shown in Fig. 2 which displays that the transmittance of ZnO is above 90% in visible region from 400 nm to 800 nm.

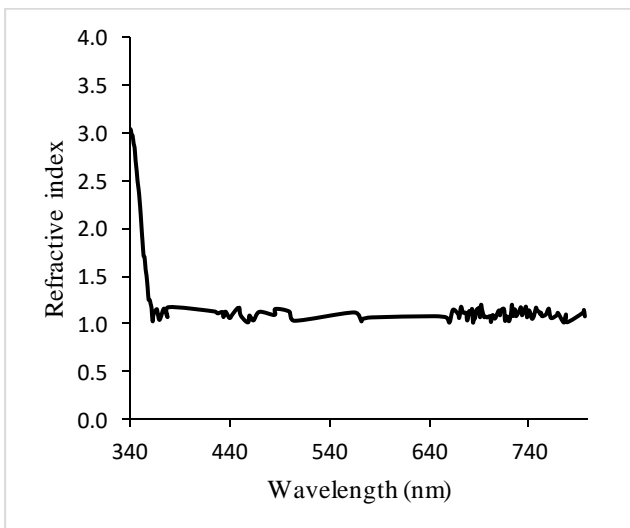


Fig. 2. Transmittance spectra of undoped ZnO

Next, the purpose of the optical properties is to determine the refractive index of ZnO that can be obtained using Equation 2.

$$n = \left[\frac{1+R^{0.5}}{1-R^{0.5}} \right] \quad (2)$$

Previous studies reported that the refractive index can be referred to the absorption edges. A considerable amount of the literature review showed that the refractive index is 2.62 at 340 nm [26]. This is in close agreement with the result obtained in this experiment which shows that the refractive index of ZnO at the absorption edge of 340 nm is about 3.0 as presented in Fig. 3. In regard to this matter, the high refractive index possess by ZnO makes it suitable for anti-reflection coatings.

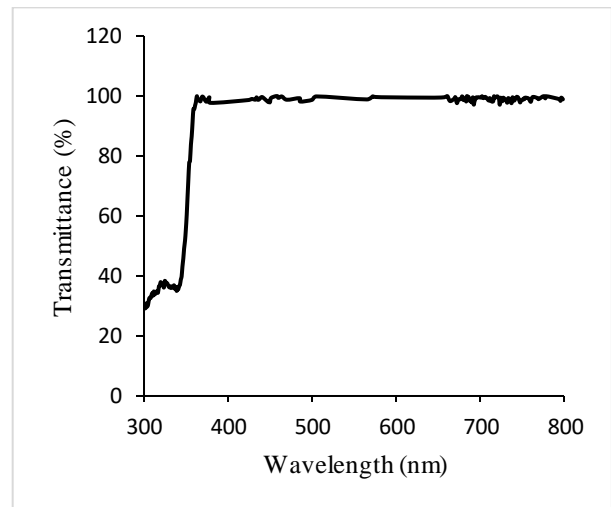


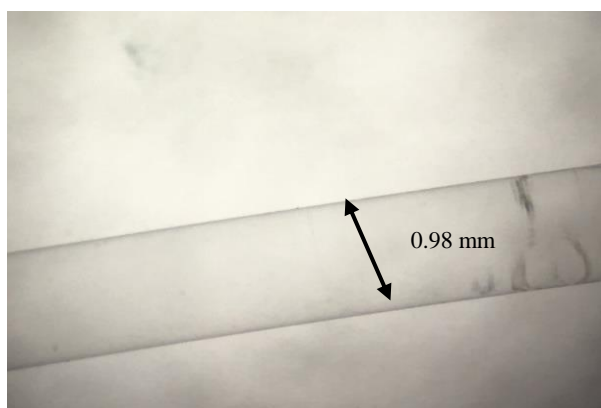
Fig. 3. Refractive index against wavelength for undoped ZnO

3.2. Etching process of polymer optical fiber

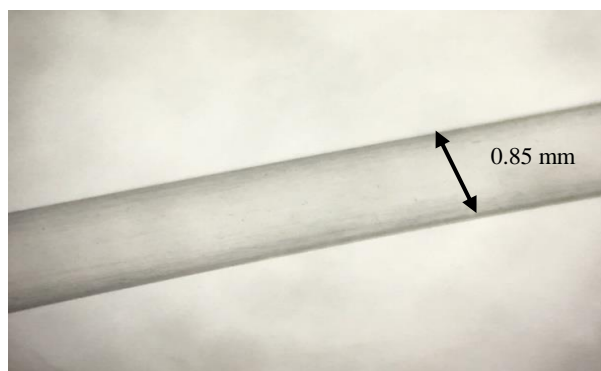
In this case, the core must be removed to allow ZnO to be coated to the unclad region after removing the jacket and cladding of POF. The etching process of unclad POF is prepared according to the chemical etching method whereby the acetone solution is used and neutralized using deionized water. The steps are continuously repeated until the waist diameter ± 0.85 mm is achieved. The initial diameter of the core is 0.98 mm according to the manufacturer of the POF known as Mitsubishi Rayon Co Ltd. Hence, the diameter of the core in this experiment is measured before and after the chemical etching process by using microscope as shown in Fig. 4. As can be observed in Fig. 4(a), the image of POF shows that the diameter of cladding is 0.98 mm after the jacket was removed. Next, the diameter of the core was measured using vernier calliper with the value of 0.85 mm after the etching process. The microscope image of etched core is shown in Fig. 4(b).

In the recent work, it was found that the diameter core ranging from 0.40 mm to 0.50 mm provides better sensitivity towards refractive index changes [27]. However, the diameter core of 0.85 mm is used in this study because POF is very sensitive to acetone which may break if over etch. Therefore, the decrement to 0.85 mm is

still acceptable because it makes POF to have higher sensitivity compared to the non-reduced core diameter.



(a)



(b)

Fig. 4. (a) Microscope image of unjacket POF fiber, (b) Microscope image of unclad POF fiber

3.3. Performance of Unclad POF coated with ZnO for measuring uric acid concentration

The unclad fiber coated with ZnO was immersed in the uric acid concentration of 100 ppm to 500 ppm following the coating and drying process, while the wavelength of optical source was fixed at 650 nm. Hence, the performance of unclad POF was evaluated based on the efficiency of 0.02 m unclad length. Next, the power output of unclad POF was compared between the coated and uncoated.

The obtained data is plotted into power output as the function of concentration as shown in Fig. 5. It is observed that the transmitted light intensity improves with the ZnO coating and linearly increases with the concentration of the uric acid solution. For 2 cm coating, the proposed sensor produces a sensitivity of 4×10^{-6} mW/ppm with a slope linearity of more than 88.56 %. Optical fiber detection relies on the evanescent wave absorption using the nanostructures coating technique [29] which is in line with the result presented in Fig. 5. As has been mentioned, the mechanism of sensing in this experiment is unclad

fiber whereby the unclad fiber will expose the evanescent field to the external sensitive coating [29].

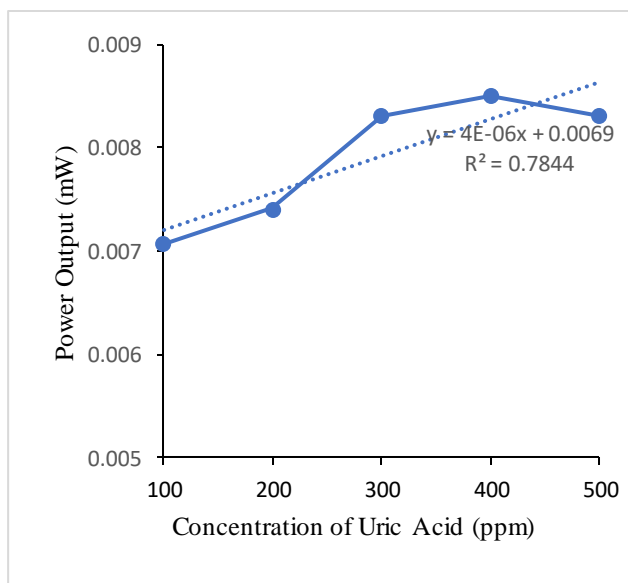
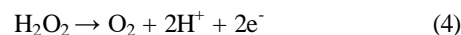


Fig. 5. Power output ratio against concentration of uric acid for ZnO coated POF at 0.02 m and 0.04 m length

On a more important note, the unclad POF enables efficient light coupling between fiber and ZnO. As shown in Fig. 6, the light is coupled into unclad POF coated with ZnO due to higher refractive index of ZnO. Refractive index for uric acid concentration of 100 ppm, 200 ppm, 300 ppm, 400 ppm and 500 ppm is 1.3331, 1.3332, 1.3334 and 1.3335 and 1.3336 respectively. Previous studies reported that the refractive index of modified cladding will increase and more evanescent field will appear in the sensing region [29]. The core and the cladding index difference drops as the refractive index of ZnO increases as the uric acid concentration increases. So the light intensity increase for ZnO coated fiber when the sensor is tested by varying the uric acid concentration.

The enzyme catalytic reaction that happens at ZnO for uric acid can be explained by the following reaction.



The electrocatalytic activity that was resulted by the good conductivity of ZnO can be credited to the production of H_2O_2 during uric acid oxidation, which then led to the generation of electron during the oxidation of H_2O_2 as shown in Equation 4. The electron produced is the key to the enhancement of light transmission, which further explains the increase in the power output of unclad POF coated with ZnO.

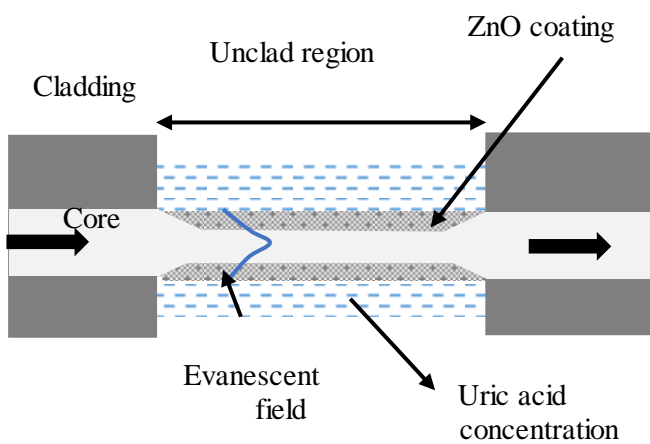


Fig. 6. Configuration of ZnO coated fiber and interaction with uric acid concentration

The power output for 2 cm and 4 cm length of uncoated fiber optic is plotted against the concentration of uric acid as shown in Fig. 7. The graph shows that the power output decreases with the concentration of uric acid. The refractive index of uric acid is larger than water and its refractive index increases as the concentration of uric acid increases. Since the cladding area has been removed, the surrounding area works as passive cladding and the light propagation depends on the refractive indexes of uric acid. The sensitivity for 2 cm unclad fiber is 2×10^{-6} mW/ppm with slope linearity of more than 90.1 %. Meanwhile, 4 cm unclad fiber shows better sensitivity of 7×10^{-6} mW/ppm with also better linearity of more than 96.32 %. Therefore, 4 cm unclad fiber allows more evanescent field to penetrate into the liquids and interact with uric acid. The longer the length of unclad fiber, the higher the evanescent wave absorbance as well as the number of reflections.

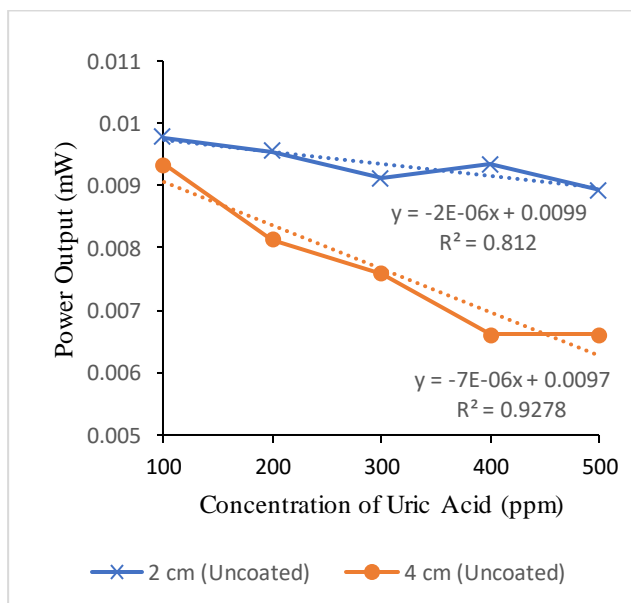


Fig. 7. Power output ratio against concentration of uric acid for uncoated POF fiber at 0.02 m and 0.04 m length

4. Conclusion

ZnO was discovered to exhibit absorption at 340 nm and transmittance around 90% at 400 nm to 800 nm which is considered to be highly transparent. The results seemed to suggest that the increase in the power output for coated POF was due to interaction between uric acid with ZnO, and the light that propagated inside the fiber. On a more important note, the sensitivity of unclad POF coated with ZnO was high because it was observed that the refractive index increases with the increase of concentration from 100 ppm to 500 ppm. Therefore, it can be concluded that the POF coated with ZnO is more efficient for uric acid detection compared to uncoated fiber. The proposed sensor provides numerous advantages such as low cost of production, simplicity of design, immune to electromagnetic interference, higher mechanical strength and ease of handling over normal silica fiber optic.

Acknowledgements

The authors would like to thank Malaysian Ministry of Education for sponsoring this work under research grants USIM/RAGS/FST/36/50215 and Universiti Sains Islam Malaysia (USIM) are also acknowledged for their guidance and support.

References

- [1] D. H. Kang, S. K. Ha, Electrolyte and Blood Pressure **12**(1), 1 (2014).
- [2] G. E. Conway, R. H. Lambertson, M. A. Schwarzmann, M. J. Pannell, H. W. Kerins, K. J. Rubenstein, M. C. Leopold, Journal of Electroanalytical Chemistry **775**, 135 (2016).
- [3] S. M. U. Ali, Z. H. Ibupoto, M. Kashif, U. Hashim, M. Willander, Sensors **12**(3), 2787 (2012).
- [4] M. Alimanesh, J. Rouhi, N. Zainal, S. Kakooei, Z. Hassan, Advanced Materials Research, 2nd International Conference on Sustainable Materials (ICoSM 2013) **795**, 616 (2013).
- [5] S. S. Kulkarni, M. D. Shirsat, International Journal of Advanced Research in Physical Science **2**(1), 14 (2015).
- [6] V. Srivastava, D. Gusain, Y. C. Sharma, Ceramics International **39**(8), 9803 (2013).
- [7] D. Zhong-Hong, Z. Rong-Jun, S. Jie, C. Yi-Ming, Z. Yu-Xiang, W. Jia-Da, C. Liang-Yao, Journal of the Korean Physical Society **55**(32), 1227 (2009).
- [8] A. R. A. Rashid, P. S. Menon, S. Shaari, Optoelectron. Adv. Mat. **7**(11-12), 835 (2013).
- [9] A. R. A. Rashid, P. S. Menon, S. Shaari, J. Nonlinear Opt. Phys. **22**(3), 1350037 (2013).
- [10] N. Jing, C. Teng, J. Zheng, G. Wang, M. Zhang, Z. Wang, Optical Fiber Technology **31**, 20 (2016).
- [11] L. Bilro, N. Alberto, J. L. Pinto, R. Nogueira, Sensors **12**, 12184 (2012).

- [12] G. Liu, D. Feng, *Optik - International Journal for Light and Electron Optics* **127**(2), 690 (2016).
- [13] K. Peters, *Smart Materials and Structures* **20**(1), 13002 (2011).
- [14] G. Wandermur, D. Rodrigues, R. Allil, V. Queiroz, R. Peixoto, M. Werneck, et al., *Biosens. Bioelectron.* **54**, 661 (2014).
- [15] M. Batumalay, F. Ahmad, A. Lokman, A. A. Jasim, S. Wadi Harun, H. Ahmad, *Sensor Review* **34**(1), 75 (2014).
- [16] S. Liehr, P. Lenke, M. Wendt, K. Krebber, M. Seeger, E. Thiele, et al., *IEEE Sens. J.* **9**, 1330 (2009).
- [17] P. Hsiao-Chun, H. H. Lu, C. Y. Li, H. S. Su, C. T. Hsu, *Opt. Express* **19**, 6749 (2011).
- [18] S. N. Elias, N. Arsad, S. A. Bakar, *Optik – International Journal for Light and Electron Optics.* <https://doi.org/10.1016/j.ijleo.2015.07.038> (2015).
- [19] A. A. Ensafi, M. Amini, *Sensors and Actuators B: Chemical* **147**, 61 (2010).
- [20] M. Batumalay, A. Lokman, F. Ahmad, H. Arof, H. Ahmad, S. W. Harun, *IEEE Sensors Journal* **13**(12), 4702 (2013).
- [21] D. Rithesh Raj, S. Prasanth, T. V. Vineeshkumar, C. Sudarsanakumar, *Optics Communications* **340**, 86 (2015).
- [22] D. S. Montero, *International Scholarly Research Network ISRN Sensor Networks* **2012**, Article ID 618136 (2012).
- [23] P. Virendra, D. Charlnene, Y. Deepti, A. J. Shaikh, V. Nandanathangam, *Spectrochimica Acta Part A* **65**, 173 (2006).
- [24] R. M. Alwan, Q. A. Kadhim, K. M. Sahan, R. A. Ali, R. J. Mahdi, N. A. Kassim, A. N. Jassim, *Nanoscience and Nanotechnology* **5**(1), 1 (2015).
- [25] M. S. S. Bose, G. Kc, *SB Academic Review* **XVI**(1), 57 (2009).
- [26] I. A. Ezenwa, *Research Journal of Chemical Sciences Res. J. Chem. Sci.* **2**(3), 2231 (2012).
- [27] S. W. Harun, M. Batumalay, H. A. Rahman, H. Ahmad, *Sensor Review* **34**(4), 13 (2014).
- [28] Y. Tian, W. Wang, N. Wu, X. Zou, X. Wang, *Sensors* **11**(4), 3780 (2011).
- [29] S. Azad, E. Sadeghi, R. Parvizi, A. Mazaheri, M. Yousefi, *Optics and Laser Technology* **90**, 96 (2017).

*Corresponding author: affarozana@usim.edu.my